Vol. 15(1), pp. 10-24, April-June, 2023
DOI: 10.5897/JGMR2023.0379
Article Number: FE007ED70605
ISSN: 2006-9766

http://www.academicjournals.org/JGMR

ACADEMIC JOURNALS
expand your knowledge

Journal of Geology and Mining Research

Full Length Research Paper

Groundwater potential and aquifer protective capacity at Nkwelle-Ezunaka Farm Estate, Southeastern Nigeria

Nzemeka Olisah C.[1], Ugwu Gabriel Z.[2*] and Onyishi George E.[2]

[1]Department of Physics and Industrial Physics, Nnamdi Azikiwe University, Awka, Nigeria.
[2]Department of Industrial Physics, Enugu State University of Science and Technology, Enugu, Nigeria.

Received 23 January, 2023; Accepted 9 March, 2023

Vertical electrical resistivity soundings (VES) were carried out at Nkwelle-Ezunaka, Southeastern Nigeria to investigate the groundwater potential and aquifer protective capacity of the area. A total of ten soundings were carried out using ABEM Terameter SAS 1000. The VES data collected were interpreted using INTERPEX software and the results presented in terms of resistivity, thickness, depth and lithology. The lithology was inferred by correlating the result to the lithology log of one of the boreholes drilled in the study area and the geology of the study area. The VES result shows lithologic layers varying from 5 to 7. Water saturated sandstone and water saturated shaly sandstone constitute the aquifer units in the area at depth of 53.6 to 124.7 m, with their thickness ranging from 52 to 102 m as shown by the isopach map. The aquifer protective capacity was determined by calculating the longitudinal conductance and matching the values to known standards. The calculated longitudinal conductance varies from 0.00009 to 0.224 mhos. The interpreted VES results reveal poor aquifer protective capacity of the overburden layers.

Key words: Longitudinal conductance, transverse resistance, isoresistivity, geoelectric layers, vertical electrical sounding, inferred lithology, contamination.

INTRODUCTION

Groundwater is the subsurface water that occurs beneath the geological formation capable of yielding water. Groundwater is constantly in motion in the hydrosphere through the process of water cycle (Amadi, 2010).

The advantages of groundwater over other sources have been severally emphasized in literatures. High percentage of water users in the world rely substantially on groundwater due to its availability in almost all parts of the world (Reilly et al., 2008). In addition, and most importantly, very minor water treatment is often required to make it potable. Groundwater is largely protected from contamination by natural barriers. However, in areas with thin weathered layers and where aquifers are in hydraulic continuity with the ground surface, groundwater could be vulnerable to contamination from surface sources.

Although water is a renewable resource, its supply in suitable quality is steadily decreasing due to poor groundwater management and effect of poor waste water management, especially in developing countries like Nigeria. The demand for groundwater resource has increased significantly throughout the world due to population growth, socio-economic development,

*Corresponding author. E-mail: gabriel.ugwu@esut.edu.ng.

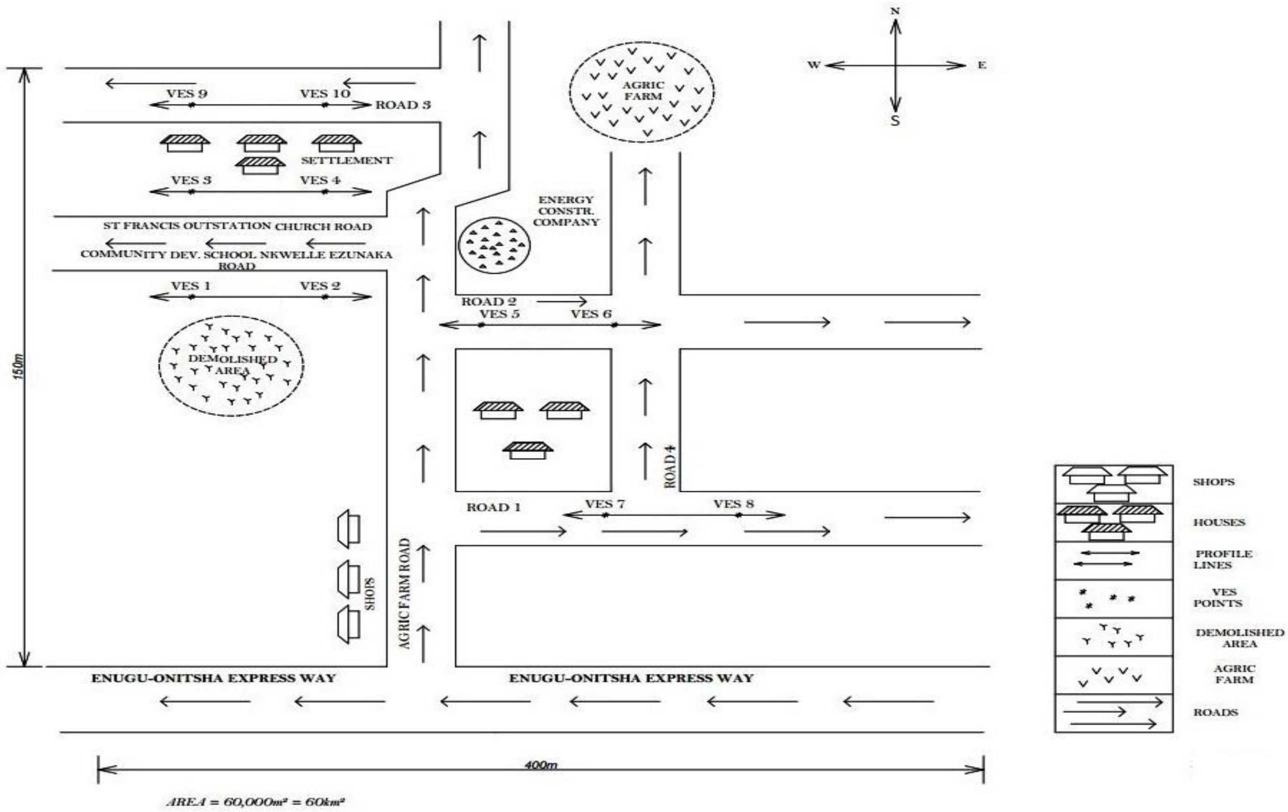

Figure 1. Sketch map of Nkwelle Ezunaka Farm Estate.
Source: Authors 2022

technological and climate changes (Olayinka et al., 1999; Alcamo, 2007). The need to sustain groundwater by people has strengthened the application of appropriate geophysical and hydrogeologic investigations (Olayinka et al., 1999; Olorunfemi et al., 1999; Lashkaripour, 2003; Batayneh, 2010; Omosuyi, 2010; Anudu et al., 2011) to locate areas of high and reliable groundwater prospect or characterize seasonal changes in the near surface aquifer (Webb et al., 2011). Water related diseases are mostly responsible for about 80% of illnesses or deaths in the developing countries (UNESCO, 2007). Though groundwater can be a source of potable water supply, there is need to evaluate its portability since it is often susceptibility to contamination.

Aquifer protective capacity has been defined as the capacity of the overburden unit to impede and filter percolating ground surface contaminating liquid into the aquifer unit. It is a measure of the ability of an earth medium to retard and filter percolating fluid. The protective capacity of an overburden is directly proportional to its thickness and inversely proportional to its hydraulic conductivity. Permeable materials such as sand and gravels have high resistivity, high hydraulic conductivity, and low longitudinal conductance while impermeable material such as clay and shale have high longitudinal conductance due to their low resistivity values. Sedimentary rocks, which usually are more porous and have high water content and low resistivity (Olisah and Obiekezie, 2020). Wet soil and fresh groundwater have even lower resistivity values. Clayey soil normally has a lower resistivity value than sandy soil.

In this study, we investigate the groundwater potential of the Nkwelle-Ezunaka Farm Estate by determining the type, thickness and protective capacity of the aquifer in the area.

Location and geology of the study area

The study area is located within Nkwelle-Ezunaka Farm Estate (Figure 1) in Oyi Local Government Area of Anambra State, Southeastern Nigeria. The area lies between longitude 6°51'27"–6°59'37"E and latitude 6°13'18"–6°20'27"N and covers an area of about 60 km^2.

The study area lies within the Anambra Basin in the Lower Benue Trough tectonic unit. Anambra Basin is a synclinal structural depression and one of the intracraton basins in Nigeria located in south central Nigeria (Figure 2). It is bounded to the north by Bida Basin and Northern Nigerian Massif, to the east by Benue Trough, to the west

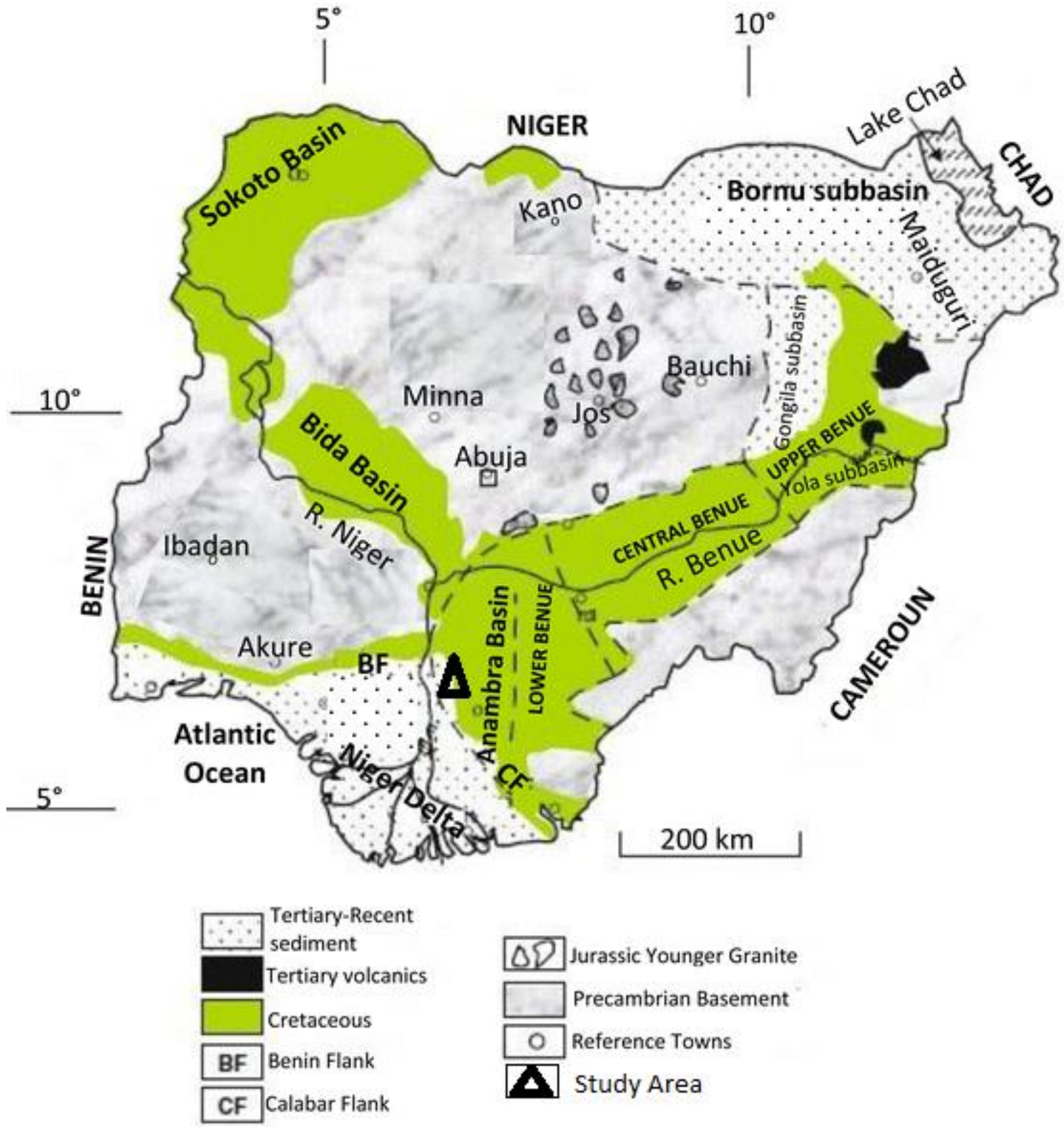

Figure 2. Geology map of the Nigeria showing the location of the study area.
Source: Obaje (2009).

by the West African Massif and to the southwest by the Niger Delta Complex (Whiteman, 1982). The basin is a Cretaceous basin having almost a roughly triangular shape (Nwajide, 1996) with a total sediment thickness of about 2500 m covering an area of about 40,000 km^2 (Reyment, 1965). Anambra Basin is characterized by enormous lithologic heterogeneity in both lateral and vertical extensions derived from a range of pale environmental setting. Anambra Basin is mainly held to have originated after the Santonian folding and uplift of the Abakaliki region during Campanian to Mid Eocene which resulted in shifting of the depocentre into Anambra Plateform and Afikpo region (Obi et al., 2001). Notable researchers (Ofoegbu, 1985; Burke, 1996) have attributed the origin of the basin to the separation of African and South America lithospheric plates and consequent opening of the Altanic in early Cretaceous. Sedimentation during the Campanian-Maastrichtian marked the beginning of deposition in the Anambra Basin and also the third cycle of marine inclusion in the Lower Benue Trough (Ehinola et al., 2005).

MATERIALS

The basic equipment used for this geophysical survey is the ABEM Terameter SAS 1000.

The resistivity meter is equipped with a 12 v battery, two current transmission cables on reels, two potential cables, four metal

Table 1. Longitudinal conductance and protective capacity rating.

Longitudinal Conductance (mhos)	Protective capacity rating
>10	Excellent
5 - 10	Very good
0.7 - 4.9	Good
0.2 - 0.69	Moderate
0.1 - 0.19	Weak
< 0.1	Poor

Source: Ogungbemi (2013).

electrodes and a salt solution. Other auxiliary equipment for the survey included a Global Positioning System (GPS) for determining the resistivity survey locations and topography, geologic hammers for driving electrodes into the ground, two measuring tapes and cutlasses for clearing the traverses.

METHODS

The study involved the use of electrical resistivity method. The technique adopted was Vertical Electrical Sounding (VES). The soundings used to characterize the various lithologic units and to determine the depth to water table. A total of ten soundings using Schlumbeger array were carried out in the area. The VES field data were processed using the Schlumberger automatic INTERPEX analysis software, which generated model curves of apparent resistivity against spacing ($\frac{AB}{2}$) using initial layer parameters. The isoresistivity, isopach and aquifer protective capacity maps of the study area were obtained using Surfer 8 software. The Dar-Zarrouk parameters were obtained from the first order geoelectric parameters (layer resistivities and thicknesses). These included the total longitudinal conductance (S) and total transverse resistance (T). These secondary geoelectric parameters are particularly important when they are used to describe a geoelectric section consisting of several layers. The longitudinal conductance is used to define target areas of groundwater potential (Okonkwo and Ugwu, 2015). High longitudinal conductance usually indicates thick succession and is suggestive of high groundwater potential. The transverse resistance has a direct relation with transmissivity and is also used to define target areas of good groundwater potential (Okonkwo and Ugwu, 2015). For n layers, the total longitudinal conductance is given as:

$$S = \sum_{i=1}^{n} \left(\frac{h_i}{\rho_i}\right) \quad (1)$$

The total transverse resistance is also given as:

$$T = \sum_{i=1}^{n} \rho_i h_i \quad (2)$$

where h_i is the thickness of the ith layer and ρi is the resistivity of the ith layer which were deduced from the VES curves of the apparent resistivity versus spacing. Using Ogungbemi (2013) classification, the results of longitudinal conductance was used to classify areas into good, moderate, weak and poor protective capacity shown in Table 1. The lithology of the layers was inferred by correlation to one of the boreholes drilled in the study area and based on the geology of the study area.

RESULTS AND DISCUSSION

Qualitative interpretation of the profiles and depth sounding curves were carried out based on distinctive geoelectric parameters of the layers represented by the four types of auxiliary curve (A, H, K and Q). VES 1, 2, 4 and 7 are type AQ curves while VES 3, 5, 6 and 10 are type KQ curves. VES 7 and 8 have type HHQ and HQ curve, respectively. VES 1, 2, 4, 5 and 7 have five geoelectric layers while VES 6, 9 and 10 have six geoelectric layers. VES 3 and 8 have seven geoelectric layers (Figures 3 to 12). A summary of qualitative interpretation of VES curves is shown in Table 2 while Table 3 shows a summary of the quantitative interpretation results of the VES.

A correlation of the interpretation results of VES 1–10 to the lithologic log of a borehole drilled in the area shows the occurrence of five, six or seven lithologic layers, namely: Lateritic silty clayey sandy top soil, lateritic sandstone, wet lateritic shale, lateritic shale, lateritic sandstone, dry sandstone, wet shale, sandstone, dry sandstone, water saturated sandstone and water saturated shaly sandstone as shown in Figures 13 to 15. The aquifer layers are water saturated sandstone and water saturated shaly sandstone. These aquifers are located either at the fourth, fifth, sixth or seventh layer (Table 3) in agreement with the result of Oyeku and Eludoyin (2010) and Uma (2003). The resistivity of the aquifer layers varies from 242.7 to 13658 Ωm (Table 3) with thickness ranging from 52 to 102 m (Figure 16). VES 2, 5 and 7 have high aquifer thickness which is a favourable condition for productive and sustainable borehole yield (Ugwu and Ezeh, 2012). The isoresistivity map of the area (Figure 17) shows that VES 4 and 10 located at the northern part of the study area have low resistivity values ranging from 1200 to 1500 Ωm, suggesting an aquiferous zone of water saturated sandstone. The aquifer layers have high transverse resistance which ranges from 36,469 to 107,117 (Table 3). This implies that the layers have high transmissivity and therefore suggests that the study area has good underground potential.

The aquifer protective capacity was determined by calculating the longitudinal conductance and was found

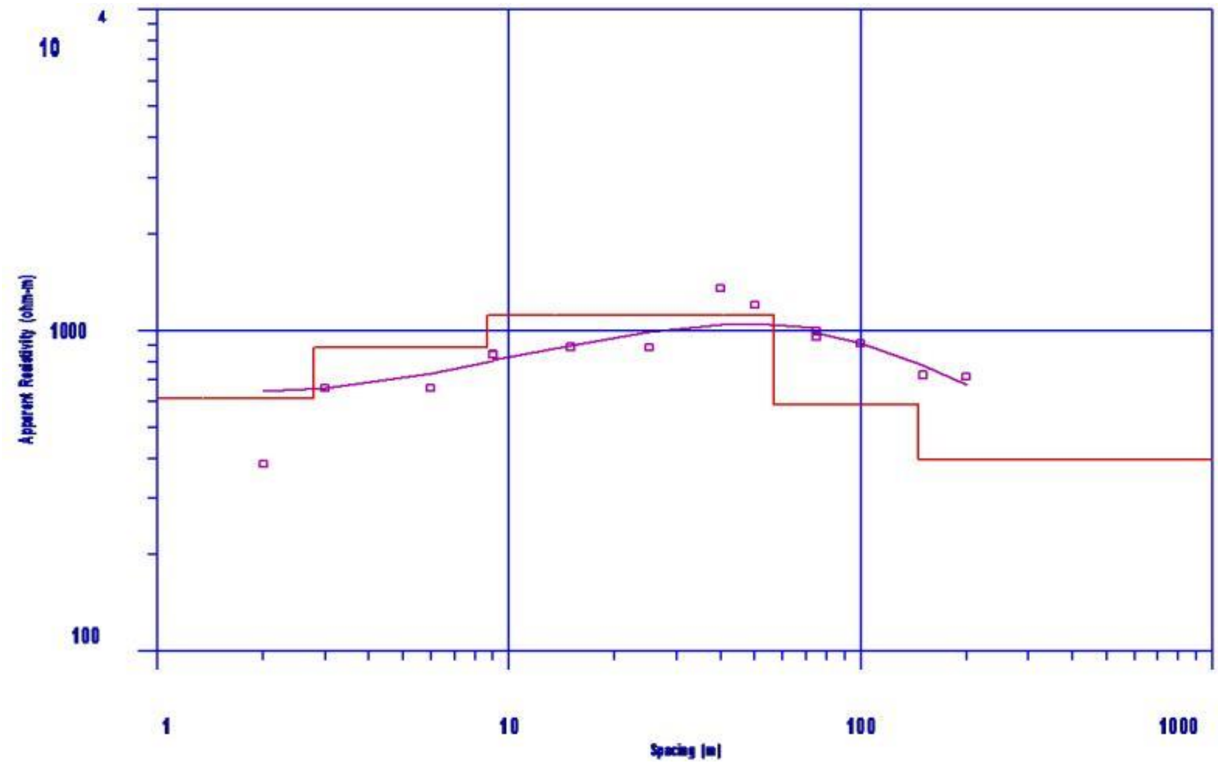

Figure 3. Interpretation result of VES 1 data.
Source: Authors 2022

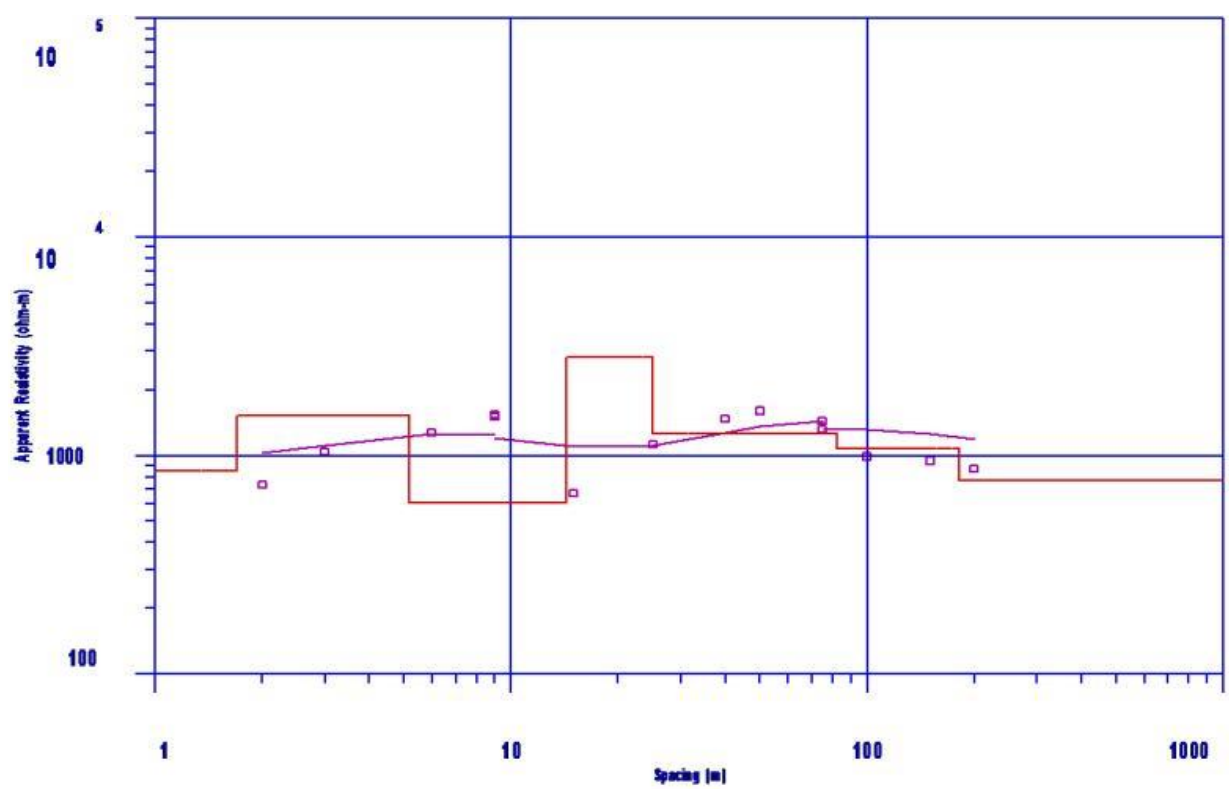

Figure 4. Interpretation result of VES 2 data.
Source: Authors 2022

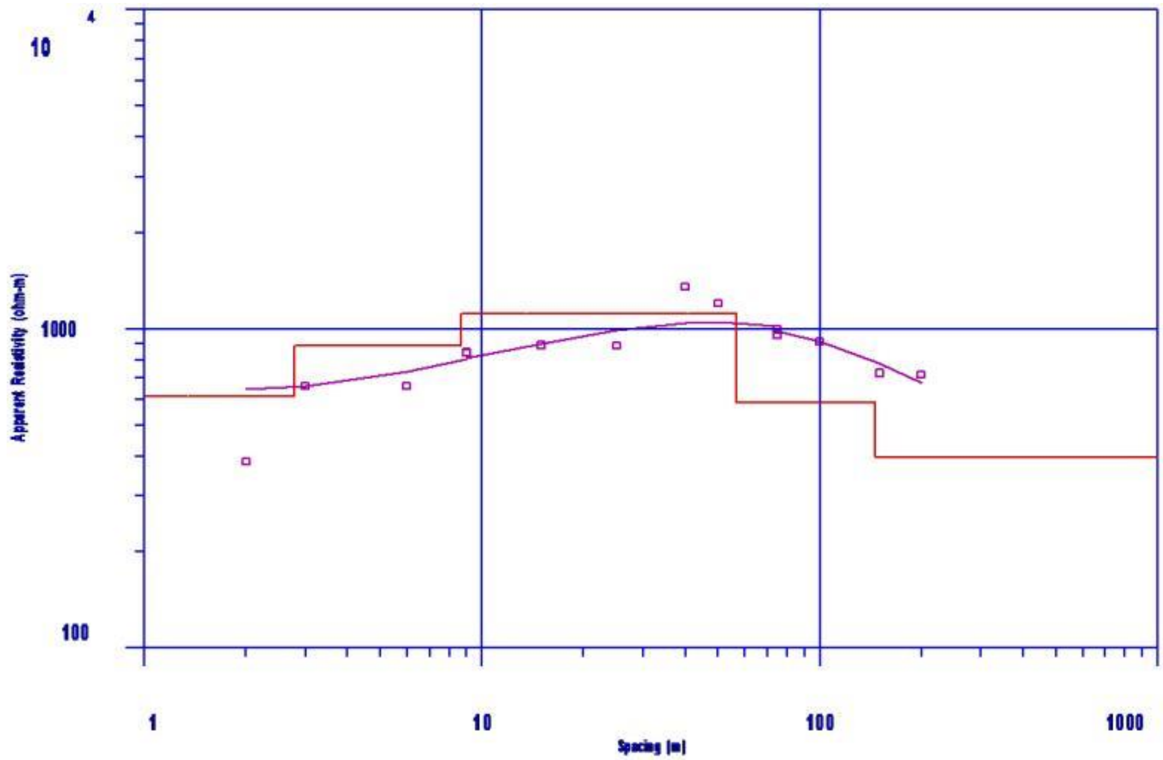

Figure 5. Interpretation result of VES 3 data.
Source: Authors 2022

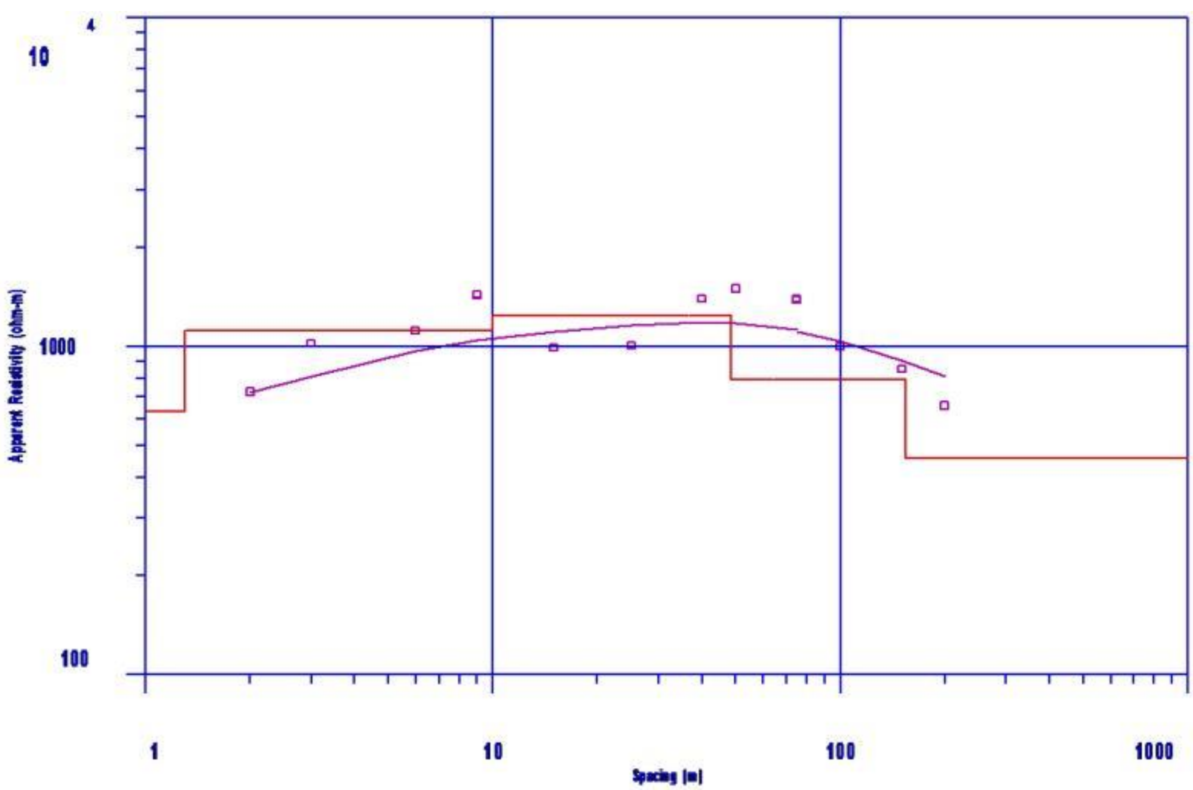

Figure 6. Interpretation result of VES 4 data.
Source: Authors 2022

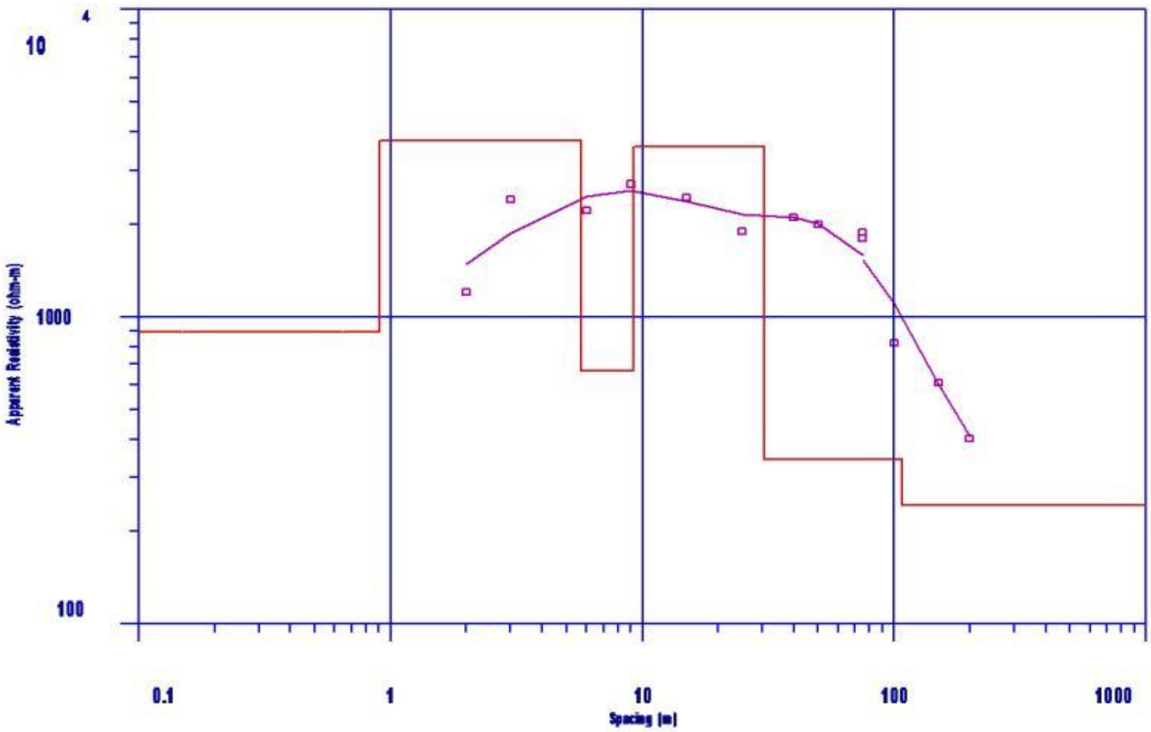

Figure 7. Interpretation result of VES 5.
Source: Authors 2022

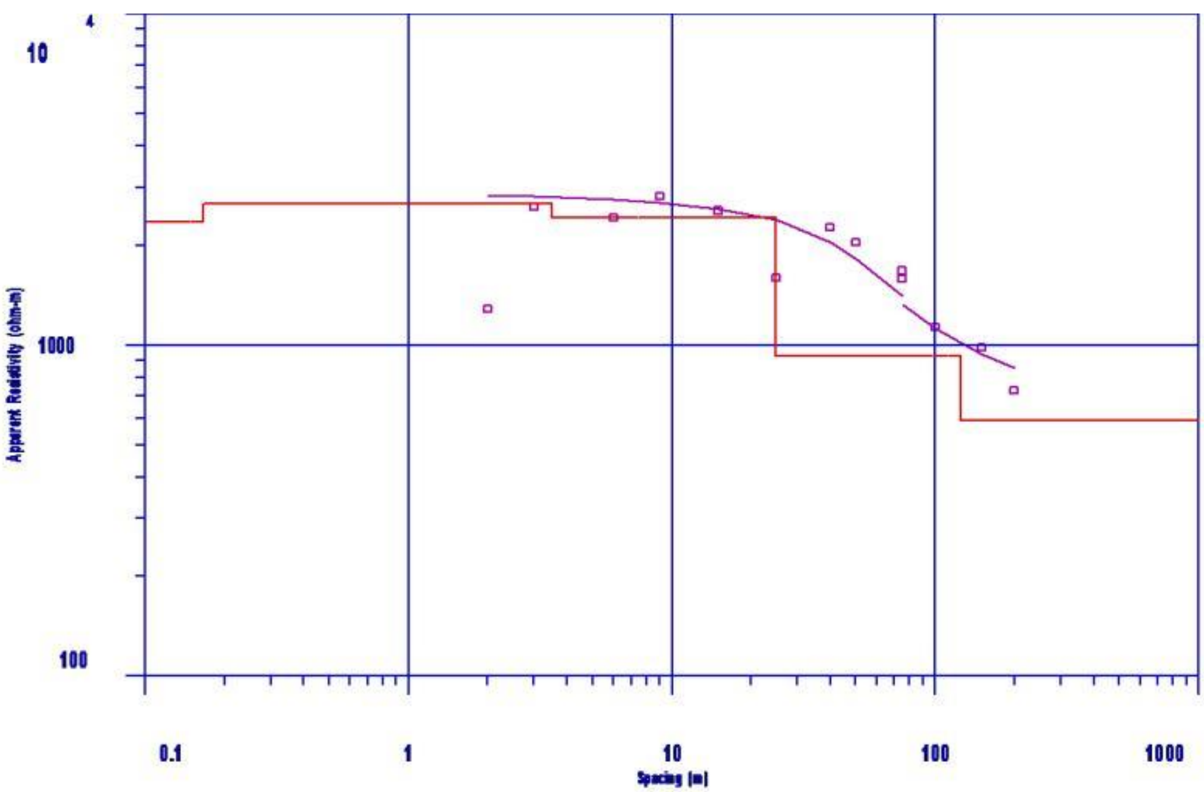

Figure 8. Interpretation result of VES 6 data.
Source: Authors 2022

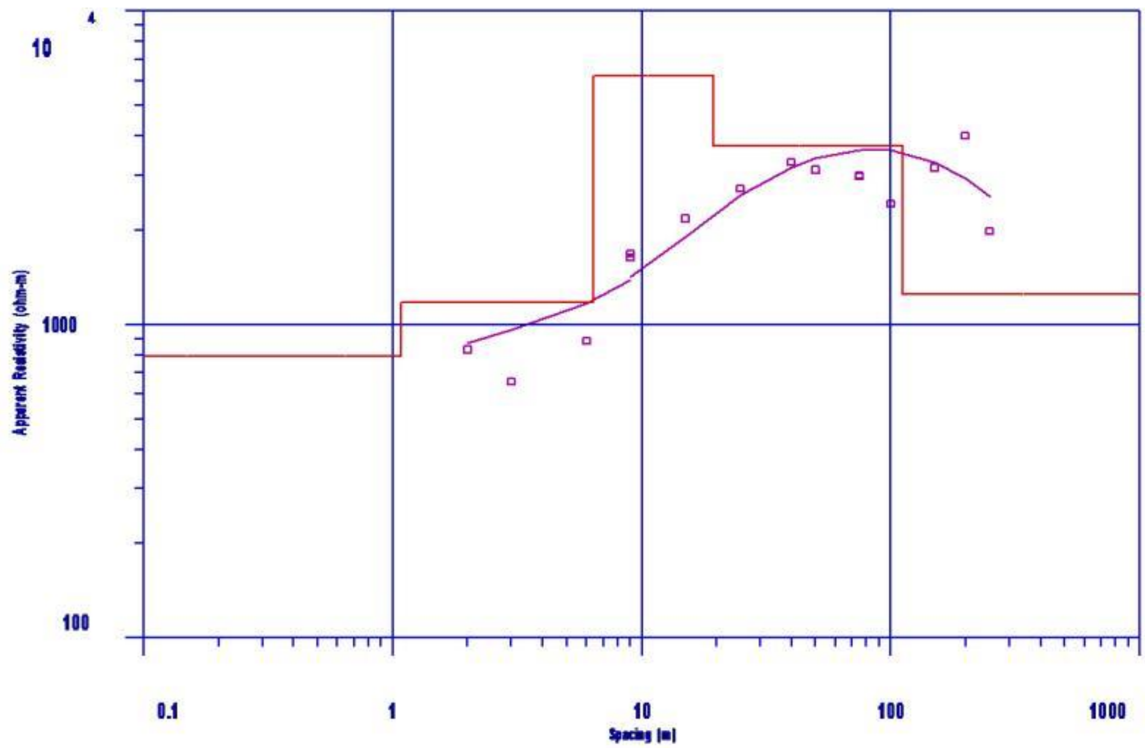

Figure 9. Interpretation result of VES 7 data.
Source: Authors 2022

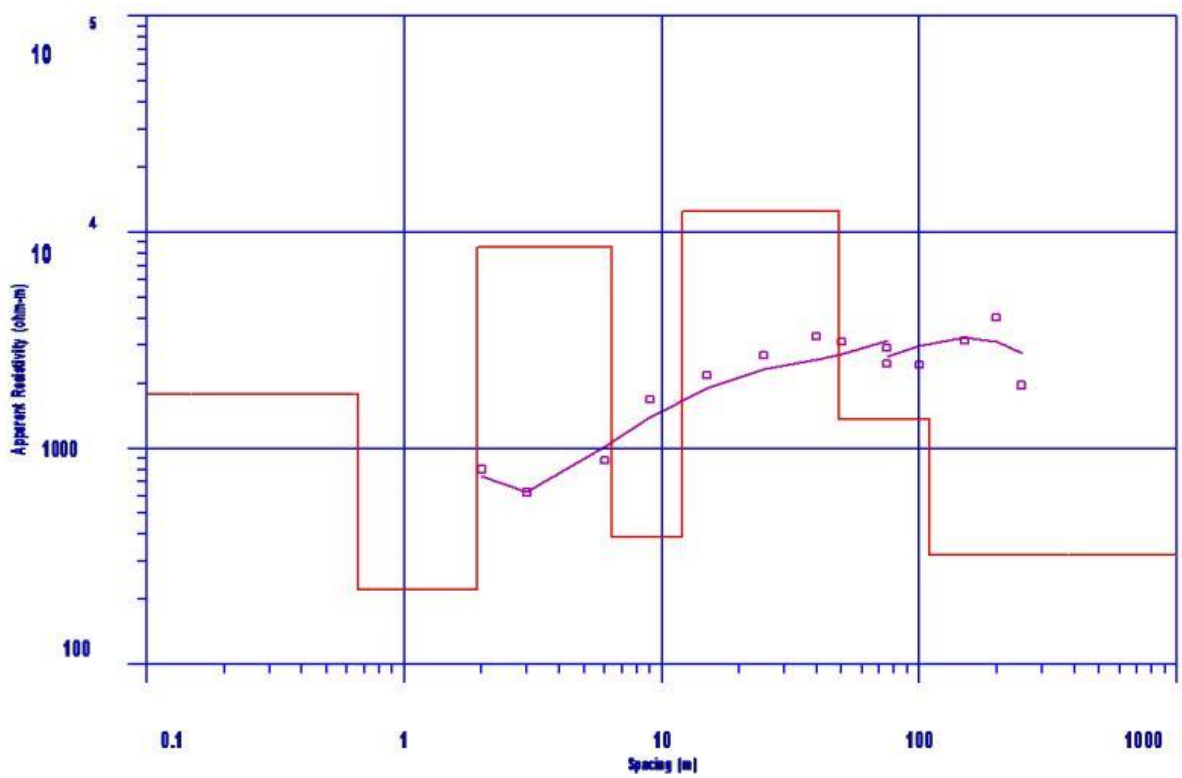

Figure 10. Interpretation result of VES 8 data.
Source: Authors 2022

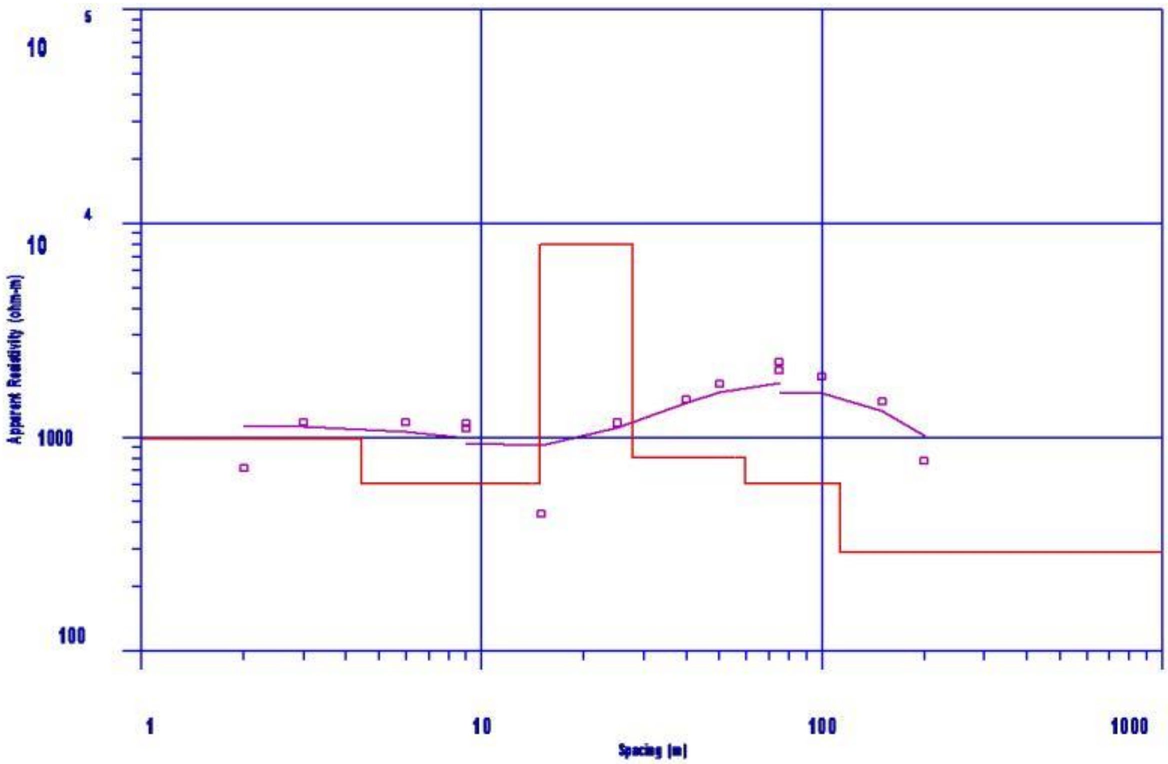

Figure 11. Interpretation result of VES 9 data.
Source: Authors 2022

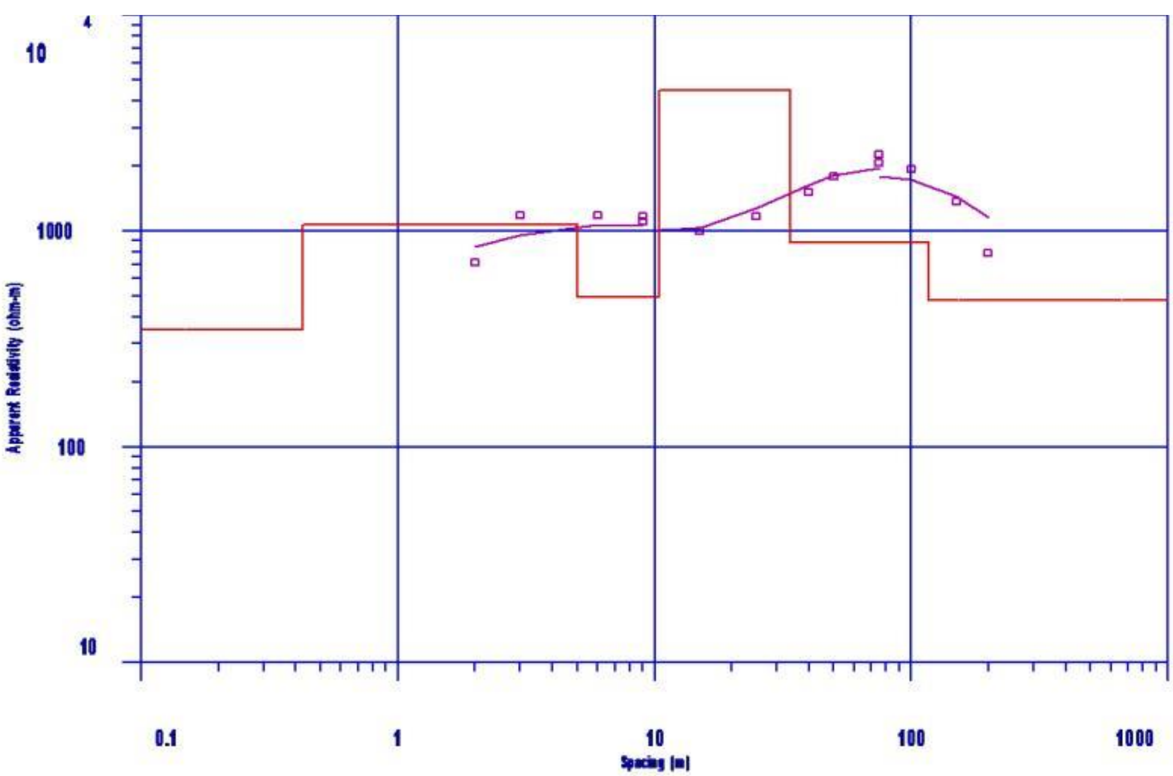

Figure 12. Interpretation result of VES 10 data.
Source: Authors 2022

Table 2. Summary of qualitative interpretation of VES curves.

VES	Coordinate	Curve type	Resistivity profile	Number of layers
1	N 6^0 16' 11'' E 6^0 51' 36''	AQ	$\rho_1<\rho_2<\rho_3>\rho_4>\rho_5$	5
2	N 6^0 16' 13'' E 6^0 55' 34''	AQ	$\rho_1<\rho_2<\rho_3>\rho_4>\rho_5$	5
3	N 6^0 18' 8'' E 6^0 51' 35''	KQ	$\rho_1<\rho_2>\rho_3<\rho_4>\rho_5>\rho_6>\rho_7$	7
4	N 6^0 18' 6'' E 6^0 55' 34''	AQ	$\rho_1<\rho_2<\rho_3>\rho_4>\rho_5$	5
5	N 6^0 15' 14'' E 6^0 57' 41''	KQ	$\rho_1<\rho_2>\rho_3>\rho_4>\rho_5$	5
6	N 6^0 15' 13'' E 6^0 59' 31''	KQ	$\rho_1<\rho_2>\rho_3<\rho_4>\rho_5>\rho_6$	6
7	N 6^0 13' 19'' E 6^0 57' 37''	AQ	$\rho_1<\rho_2<\rho_3>\rho_4>\rho_5$	5
8	N 6^0 13' 18'' E 6^0 59' 37''	HHQ	$\rho_1>\rho_2<\rho_3>\rho_4<\rho_5>\rho_6>\rho_7$	7
9	N 6^0 20' 27'' E 6^0 51' 27''	HQ	$\rho_1>\rho_2<\rho_3>\rho_4>\rho_5>\rho_6$	6
10	N 6^0 20' 28'' E 6^0 55' 27''	KQ	$\rho_1<\rho_2>\rho_3<\rho_4>\rho_5>\rho_6$	6

Source: Authors 2022

Table 3. Summary of quantitative interpretation of VES results.

VES	Layer	ρ (Ωm)	Thickness (m)	Depth (m)	Lithology	Longitudinal conductance (S) (mhos)	Transverse resistance (T)	Aquifer Protective Capacity
	1	614.4	2.8	2.8	Lateritic silty, clayey sandy top soil	0.0046	1720.32	
	2	886.3	5.9	8.7	Lateritic sandstone	0.0067	5229.17	
1	3	1113.9	48.1	56.8	Sandstone	0.0431	53578.59	(0.0544) Poor
	4	587	88.6	145.4	Water saturated sandstone	0.1509	52008.2	
	5	395.1	∞	∞	Water saturated shaly sandstone	∞	∞	
	1	323.3	1.2	1.2	Lateritic silty, clayey sandy top soil	0.0037	387.96	
	2	837.7	5.9	7.1	Lateritic sandstone	0.0070	4942.43	
2	3	1375.7	36.1	43.2	Sandstone	0.0262	49662.77	(0.0369) Poor
	4	658.5	124.7	167.9	Water saturated sandstone	0.1894	82114.95	
	5	532.1	∞	∞	Water saturated shaly sandstone	∞	∞	
	1	854.8	1.7	1.7	Lateritic silty, clayey sandy top Soil	0.0020	1453.16	
3	2	1517.4	3.5	5.2	Lateritic sandstone	0.0023	5310.9	(0.0691) Poor
	3	608.4	9.2	14.3	Lateritic shale	0.0151	5597.28	
	4	2814.5	10.7	25.0	Dry sandstone	0.0038	30115.15	

Table 3. Cont'd

	5	1253.7	57.5	82.5	Sandstone	0.0459	72087.75	
	6	1080.9	99.1	181.6	Water saturated sandstone	0.0917	107117.19	
	7	768.8	∞	∞	Water saturated shaly sandstone	∞	∞	
4	1	630.8	1.3	1.3	Lateritic silty, clayey sandy top soil	0.0021	820.04	(0.041) Poor
	2	1117.7	8.7	10.0	Lateritic sandstone	0.0078	9723.99	
	3	1241.9	38.6	48.6	Sandstone	0.0311	47937.34	
	4	791.7	105.1	153.7	Water saturated sandstone	0.1327	83207.67	
	5	455.3	∞	∞	Water saturated shaly sandstone	∞	∞	
5	1	2352.1	0.2	0.2	Lateritic silty, clayey sandy top Soil	0.00009	470.42	(0.01009) Poor
	2	2680.0	3.3	3.5	Lateritic sandstone	0.0012	8844	
	3	2426.2	21.3	24.8	Sandstone	0.0088	51678.06	
	4	925.3	100.6	125.4	Water saturated sandstone	0.1087	93085.18	
	5	591.7	∞	∞	Water saturated shaly sandstone	∞	∞	
6	1	888.8	0.9	0.9	Lateritic silty, clayey sandy top soil	0.0010	799.92	(0.0137) Poor
	2	3741.9	4.8	5.7	Lateritic sandstone	0.0013	17961.12	
	3	664.5	3.6	9.3	Shaly sandstone	0.0054	2392.2	
	4	3570.0	21.3	30.6	Sandstone	0.0060	76041	
	5	344.0	76.5	107.1	Water saturated Sandstone	0.2224	26316	
	6	242.7	∞	∞	Water saturated shaly-sandstone	∞	∞	
7	1	791.7	1.1	1.1	Lateritic silty, clayey sandy top soil	0.0014	870.87	(0.0329) Poor
	2	1177.1	5.4	6.4	Lateritic sandstone	0.0046	6356.34	
	3	6183.8	13.0	19.5	Dry sandstone	0.0021	80389.4	
	4	3700.2	91.9	111.3	Sandstone	0.0248	340048.38	
	5	1246.2	∞	∞	Water saturated sandstone	∞	∞	
8	1	1782.4	0.7	0.7	Lateritic silty, clayey sandy top soil	0.00039	1247.68	(0.02372) Poor
	2	221.0	1.2	1.9	Wet lateritic shale	0.0054	265.2	
	3	8507.5	4.5	6.4	Lateritic sandstone	0.00053	38283.75	
	4	389.2	5.6	12.0	Wet shale	0.0144	2179.52	
	5	12413.5	36.9	48.9	Dry sandstone	0.0030	458058.15	
	6	1365.8	60.5	109.4	Water saturated sandstone	0.0443	82630.9	
	7	321.4	∞	∞	Water saturated shaly-sandstone	∞	∞	
9	1	982.5	4.4	4.4	Lateritic silty, clayey sandy top soil	0.0045	4323	(0.0624) Poor
	2	608.4	10.4	14.8	lateritic sandstone	0.0171	6327.36	
	3	7976.3	13.0	27.9	Dry Sandstone	0.0016	103691.9	
	4	802.0	31.4	59.3	Sandstone	0.0392	25182.8	
	5	608.4	53.6	112.9	Water saturated sandstone	0.0881	36469.44	
	6	289.1	∞	∞	Water saturated shaly-sandstone	∞	∞	
10	1	348.9	0.4	0.4	Lateritic silty, clayey sandy top Soil	0.0011	139.56	(0.0218) Poor
	2	1065.5	4.6	5.0	lateritic sandstone	0.0043	4901.3	
	3	491.0	5.5	10.5	Lateritic shale	0.0112	2700.5	
	4	4468.9	23.3	33.8	Dry sandstone	0.0052	104125.37	
	5	887.6	83.1	116.8	Water saturated sandstone	0.0936	73759.56	
	6	478.9	∞	∞	Water saturated shaly sandstone	∞	∞	

Source: Authors 2022

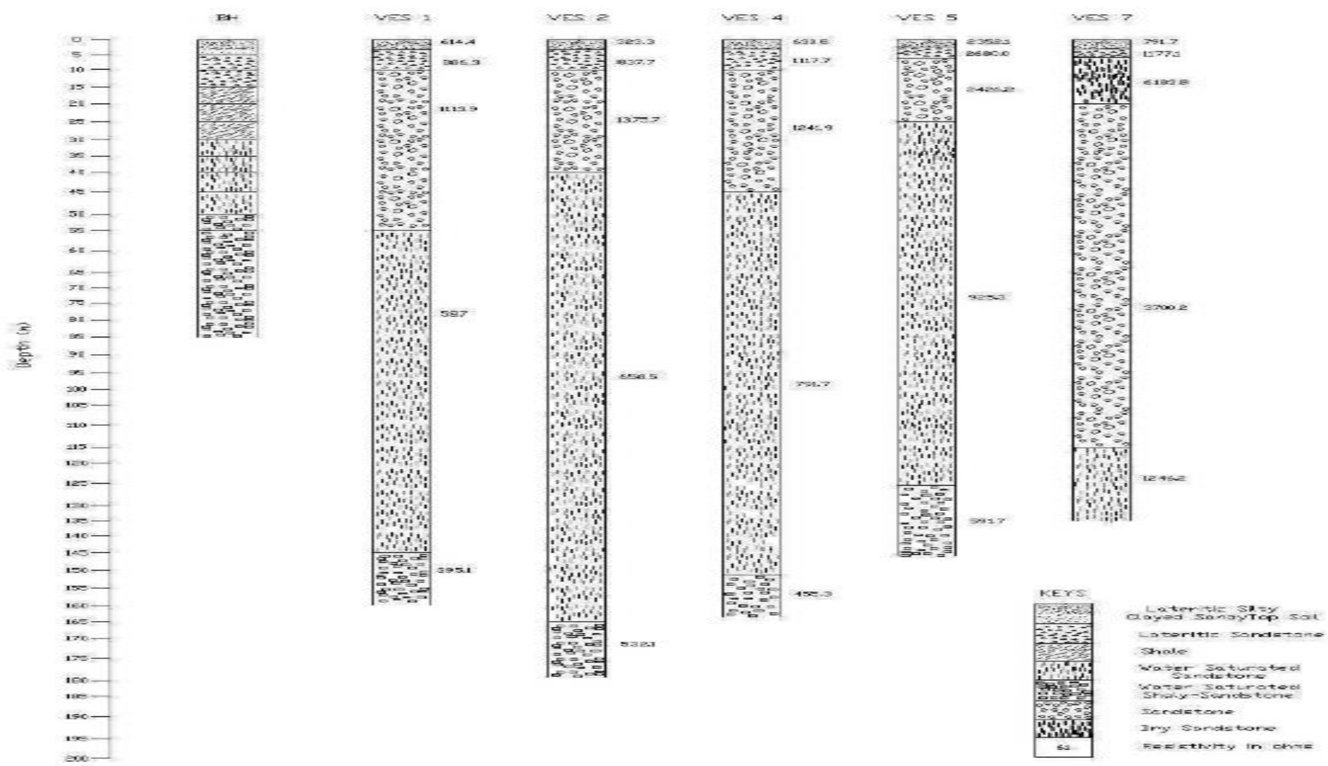

Figure 13. Interpreted lithology of the five layer VES curves.
Source: Authors 2022

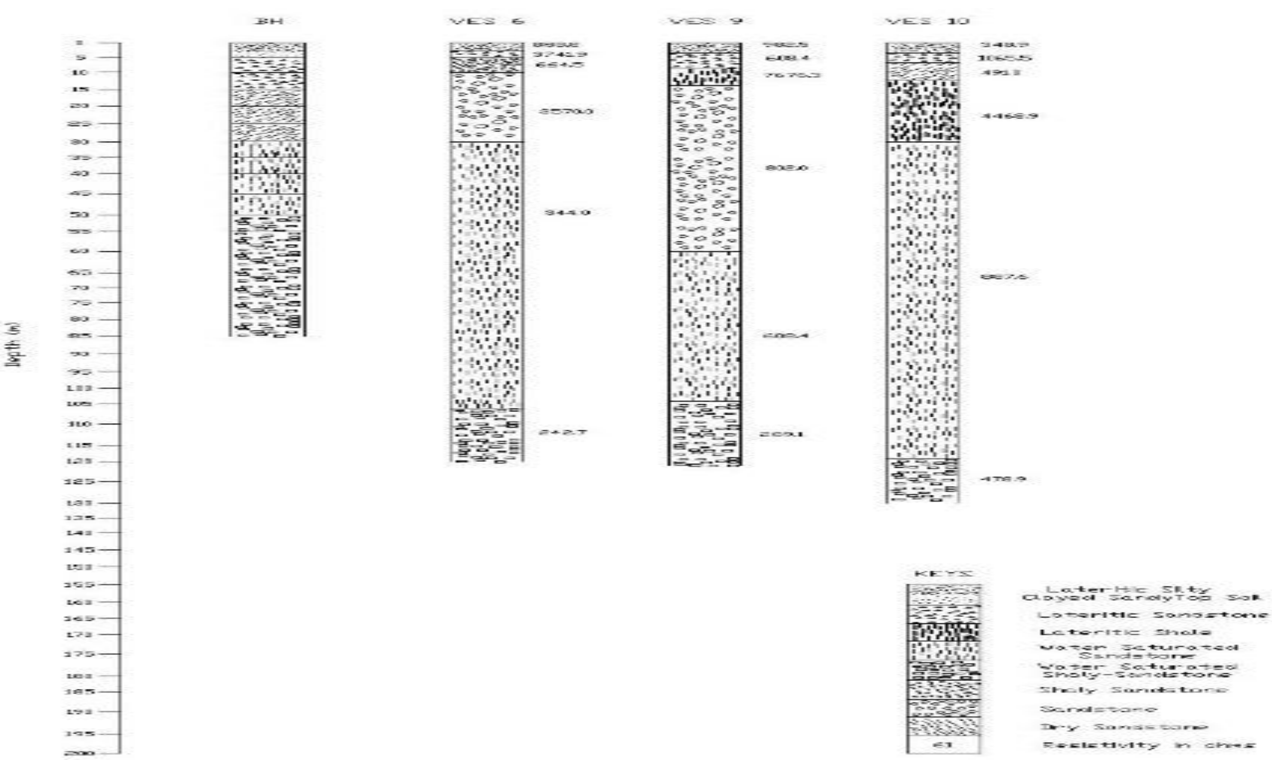

Figure 14. Interpreted lithology of the six layer VES curves.
Source: Authors 2022

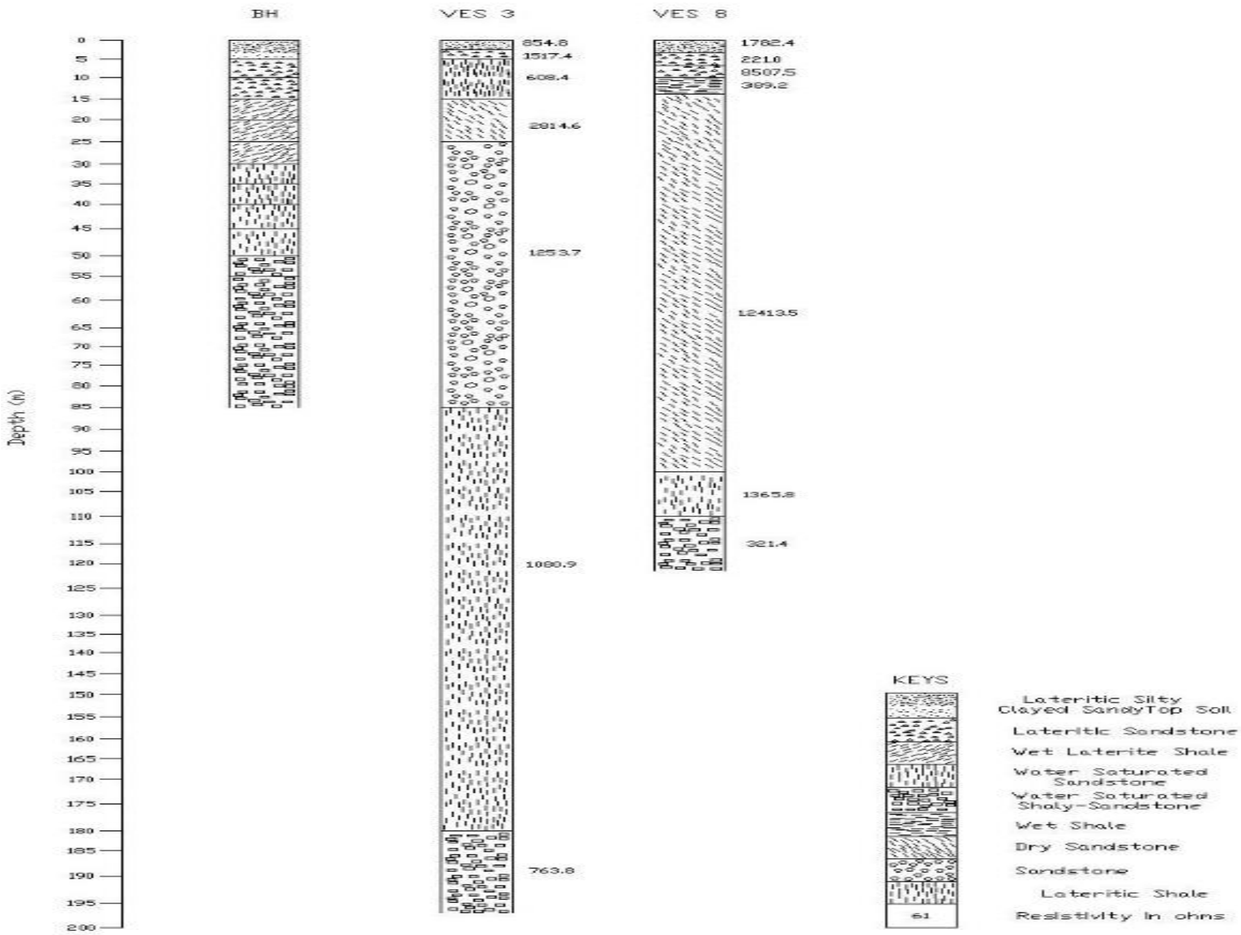

Figure 15. Interpreted lithology of the seven layer VES curves.
Source: Authors 2022

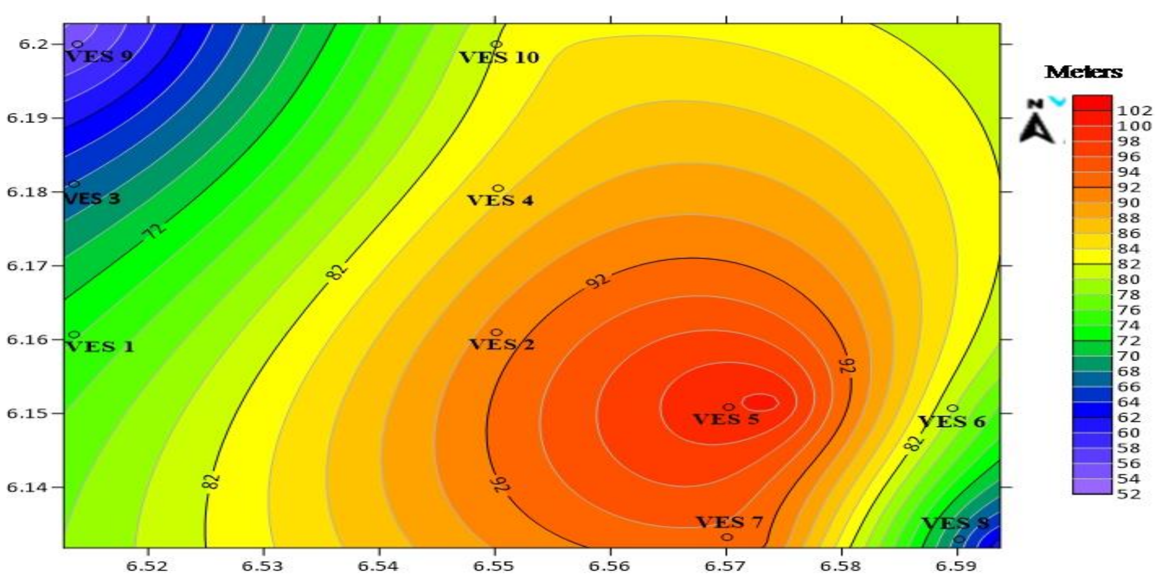

Figure 16. Isopach (thickness) map of the aquifer layers at various VES stations.
Source: Authors 2022

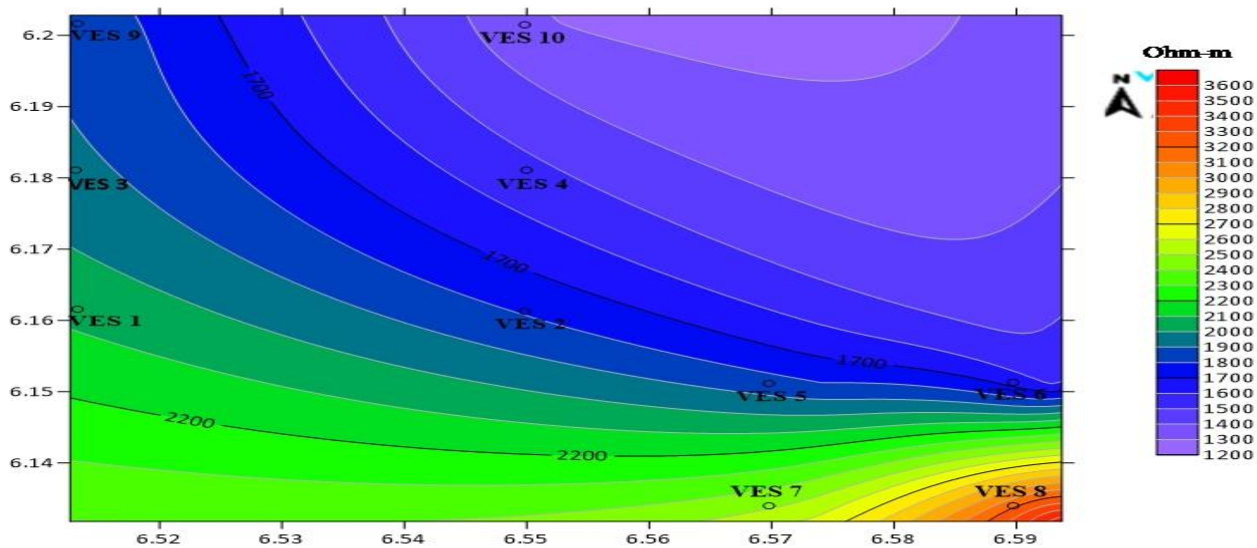

Figure 17. Isoresistivity map of the study area.
Source: Authors 2022

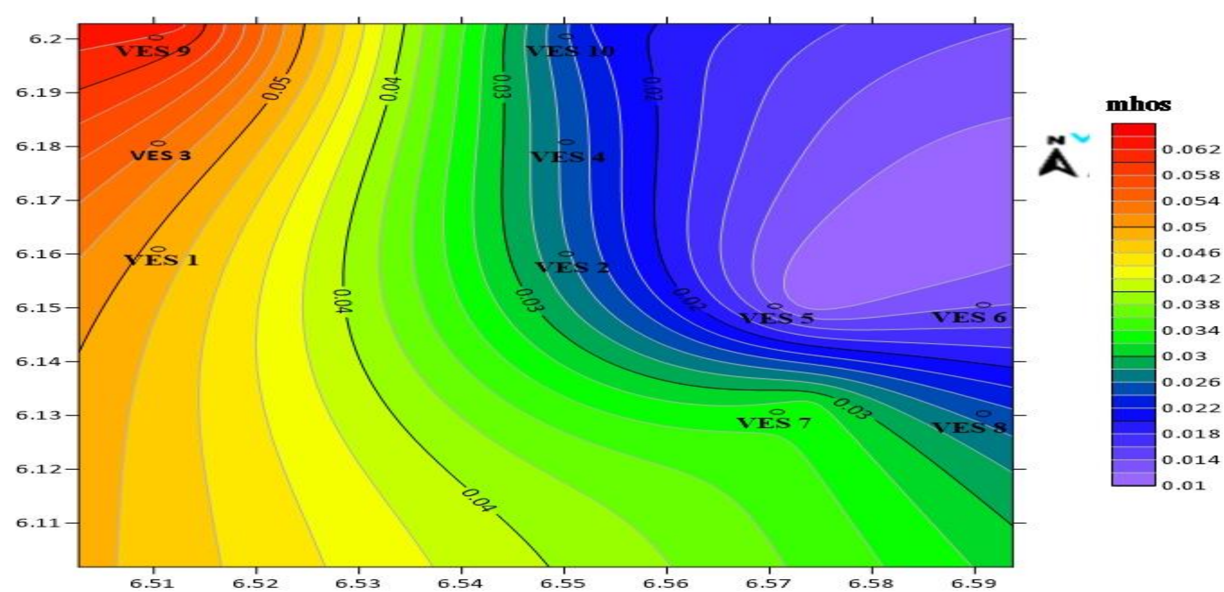

Figure 18. Map of aquifer protective capacity of the study area.
Source: Authors 2022

to vary from 0.0 to 0.062 mhos as shown in Figure 18. This range indicates a poor aquifer protective capacity, in accordance with Ogungbemi (2013).

Conclusion

In this study, the groundwater prospect and aquifer protective capacity of the rock units at Nkwelle-Ezunaka Farm Estate in Southeastern Nigeria were investigated by conducting ten vertical electrical soundings. The results showed that VES 1, 2, 4, 5 and 7 have five lithologic layers, VES 6, 9 and 10 have six geoelectric layers while VES 3 and 8 have seven lithologic layers. The subsurface sequence comprises the lateritic silt, clayey sandy topsoil, lateritic sandstone, sandstone, dry sandstone, lateritic shale, water saturated sandstone and water saturated shaly sandstone. The water saturated sandstone and water saturated shaly sandstone layers constitute the aquifer units in the area, with depth ranging from 53.6 to 124.7 m, and thickness varying from 52 m to a maximum of 102 m. VES 2, 5 and 7 stations have been identified as the best locations for productive and sustainable borehole yield because of their high aquifer thicknesses and transmissivity.

This study also revealed that all parts of the area are underlain by materials of poor protective capacity, implying that the area is vulnerable to contamination that may arise from runoff water, sewage and indiscriminately disposed waste materials in the area. Thus, the information obtained from this study can serve as a baseline data for pre-drill estimate of yield of any prospective borehole in the area.

CONFLICT OF INTERESTS

The authors have not declared any conflict of interests.

REFERENCES

Alcamo J (2007). Future long-term changes in global water resources driven by socioeconomic and climatic changes. Hydrological Sciences Journal 52(2):247-275.

Amadi AN (2010). Effects of Urbanization on groundwater quality. A case study of Port Harcourt Southern Nigeria. Natural Applied Science ISSN 1119-9296: 11(2):43-152.

Anudu GK, Onuba LN, Ufondu LS (2011). Geoelectric sounding for groundwater exploration in the crystalline basement terrain around Onipe and adjoining areas, Southwestern Nigeria. Journal of applied technology in environmental sanitation 1(4):343-354.

Batayneh AT (2010). Mapping Quaternary deposits in the El-Jufr playa (Southwestern Jordan plateau) using geoelectrical techniques: implications for geology and hydrogeology. Science Research Essays 5(20):3183-3192.

Burke KC (1996). Geological history of Benue Trough and adjacent area. In Dessauvagie, TFJ. and Whiteman AJ (eds.), African Geology. Univ. of Ibadan Press Nigeria pp. 187-218.

Ehinola OA, Sonibare OO, Falode OA, Awofale BO (2005). Hydrocarbon potential and thermal maturity of Nkporo shale from Lower Benue Trough, Nigeria. Journal of Applied Sciences 5(4):689-695.

Lashkaripour GR (2003). An investigation of groundwater condition by geoelectric resistivity method: a case study in Korin aquifer, Southeast Iranian, Journal of Spatial Hydrology 3(1):1-5.

Nwajide CS (1996). Eocene tidal sedimentation in the Anambra Basin, Southern Nigeria. Sedimentary Geology 25:189-207.

Obi GC, Okogbue CO, Nwajide CS (2001). Evolution of the Enugu Cuesta: a tectonically driven erosional process. Global Journal of Pure Applied Sciences 7:321-330.

Ofoegbu CO (1985). A review of the geology of the Benue Trough, Nigeria. Journal of African Earth Science 3:283-291.

Ogungbemi SO (2013). Longitudinal Conductance/Protective Capacity Rating. Journal of Applied Geology and Geophysics 1(5):1-7.

Okonwo A, Ugwu, GZ (2015). Determination of Dar-Zarrouk parameters for prediction of aquifer protective capacity: case study of Agbani sandstone aquifer, Southeastern Nigeria.

Olayinka AI, Abimbola AF, Isibor RA, Rafiu AR (1999). A geoelectrical hydrogeochemical investigation of shallow groundwater occurrence in Ibadan, Southwestern Nigeria. Environmental geology 37(1-2):31-39.

Olisah NC, Obiekezie TN (2020). An investigation of groundwater contamination around Nsukka municipality dumpsite using resistivity method. Scienceopen 1:22-33.

Olorunfemi MO, Ojo JS, Akintunde OM (1999). Hydrogeophysical evaluation of the groundwater potentials of Akure metropolis, Southwestern Nigeria. Journal of Mining and Geology 35(2):207-228.

Omosuyi GO (2010). Geoelectric assessment of groundwater prospect and vulnerability of overburden aquifers at Idanre, Southwestern Nigeria. Journal of Applied Science 3(1):19-28.

Oyeku OT, Eludoyin AO (2010). Heavy metal contamination of groundwater resources in a Nigerian urban settlement. African Journal of Environmental Science and Technology 4(4):201-214.

Reilly T, Dennehy KF, Alley WM, Cunningham WL (2008). Groundwater availability in the United State. US Geological Society Circular 1323:70.

Ugwu GZ, Ezeh CC (2012). Estimation of aquifer characteristics using vertical electrical sounding (VES) data from Enugu State University of Science and Technology, Agbani, Nigeria. International Journal of Physical Sciences 7(49):6255-6262.

Uma KO (2003). Hydrogeology of the perched aquifer systems in the hilly terrains of Nsukka town, Enugu State, Nigeria, Water Resources Journal 14:85-92.

UNESCO (2007). Record of illness and death from Water related diseases in the developing countries. Journal of Medical Ethics 33(3):150-154.

Webb SJ, Ngobeni D, Jones M, Abive T, Devkurran N, Goba R, Ashwal LD (2011). Hydrogeophysical investigation for groundwater at the Dayspring children’s village, South Africa, Leading Edge 30(4):434-440.

Whiteman A (1982). Nigeria: its petroleum geology, resources and potential. Graham and Trotman 2:394.